京都大学防災研究所年報 第 68 号 B
DPRI Annuals, No. 68 B, 2025

Preliminary Report on Broadband Magnetotelluric Survey on Sakurajima Island

Cinantya Nirmala DEWI(1), Ryokei YOSHIMURA, Maki HATA, Rintaro MIYAMACHI, Shintaro KOMATSU, Ken'ichi YAMAZAKI, Tadaomi SONODA and Yuusuke TAKENAKA

(1) Graduate School of Science, Kyoto University, Japan

Synopsis

A broadband magnetotelluric (MT) survey was conducted at 35 sites to image the subsurface structure and reveal the magmatic system of Sakurajima volcano. We performed the initial data analysis to evaluate the dimensionality and sounding resistivity of the structure. The phase tensor analysis indicates that the Sakurajima Island subsurface main structure tends in a northeast-southwest direction. In addition, the induction vector analysis at 7.111 s detects good conductors in the Northeast of Sakurajima and around Minamidake and/or Showa craters. The 1D models indicate that the near-surface resistivity structures on Sakurajima Island exhibit high resistivity, underlain by low resistivity, and then high resistivity in the deeper part. The conductive zone may be related to the magma plumbing system. In the future, we will perform 2D and 3D modeling to confirm the 1D result and obtain a more reliable estimation of the magmatic system distribution on Sakurajima Island.

Keywords: volcano magmatism, electromagnetic method, sounding resistivity

1. Introduction

Sakurajima is a stratovolcano located south of Aira Caldera in Kyushu Island, Japan. It has three craters, namely Kitadake, Minamidake, and Showa. The Vulcanian eruption has repeatedly occurred at Minamidake crater since 1955 and shifted to Showa crater in June 2006. Recently, eruptive activities have occurred both in Minamidake and Showa craters (Yamaoka et al., 2014; Permana et al., 2022).

To assess Sakurajima volcanic activity, it is important to have a better understanding of its volcanic system. One of the reliable techniques for mapping the deep volcanic subsurface structure is a magnetotelluric (MT) survey. MT is a passive sounding method that simultaneously records the natural variation of the Earth's electric and magnetic fields (Simpson and Bahr, 2005). The resistivity anomaly from MT data will provide valuable information on deep volcanic structure. In a volcanic area, the resistive zone is typically correlated with the volcanic-geothermal zone and its magmatic system (Hill et al., 2015).

Previous studies using MT and Audio Magnetotelluric (AMT) methods on Sakurajima have pointed out that the resistive zone beneath Sakurajima Island is correlated with the magmatic structure (Kanda et al., 2011; Aizawa et al., 2013). However, the previous AMT sounding depth was shallow, and the number of sites from the MT survey was limited. These lead to limited resolution of the resistivity distribution corresponding to the Sakurajima volcanic system. Therefore, we conducted a new MT survey on Sakurajima Island with more sites and deeper penetration. Our study

aims to clarify the magmatic system of the Sakurajima volcano. This preliminary study focused on obtaining an initial overview of subsurface structure analysis on Sakurajima Island based on phase tensor, induction vector, and 1D inversion analyses.

2. Methods

Broadband MT measurements were carried out at Sakurajima Island from October 29, 2024 to March 11, 2025. We used the ELOG-MT/PHX/DUAL systems (NT System Design Inc.) to record electromagnetic fields at 2,400 Hz, 150 Hz, and 15 Hz sampling frequencies. Induction coil sensors (MTC-50/80H Phoenix Geophysics Ltd.) and lead-lead chloride electrodes (WL Wolf Chemical Ltd./PB-90G Ask System Inc.) were used to measure magnetic and electric fields, respectively. We have 35 observation sites on Sakurajima Island, consisting of 17 full-component sites and 18 two-component sites, as shown in Fig. 1. The detailed location and recording time of each site are listed in Table 1.

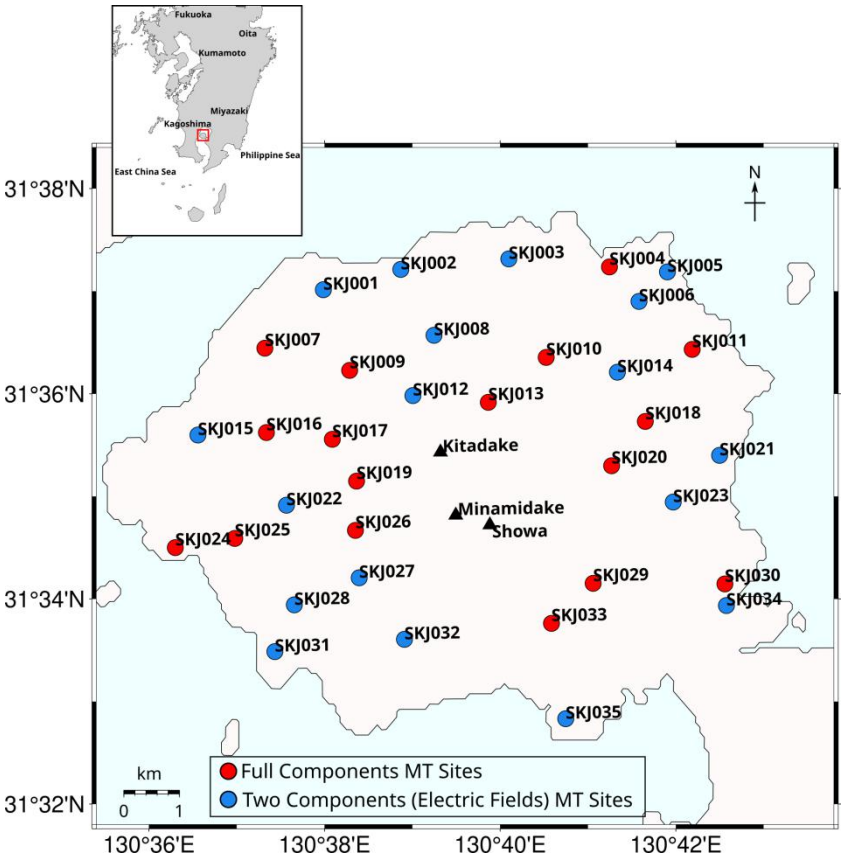

Fig. 1 Map of MT sites on Sakurajima Island

The time series data was carefully checked to ensure data quality. We chose nighttime data from 15.00 to 19.00 UTC for 150 Hz and 15 Hz data, and 17.00 UTC for 2,400 Hz data, to avoid artificial noise while reducing data capacity and processing time. However, we still found artificial noise around the commercial frequency band and periodic noise around 0.1 Hz at 12 sites. Therefore, we applied notch filters at frequencies around 60 Hz and 0.1 Hz to improve data quality. The filtered time series data was used as an input for the Bounded Influence Remote Reference Processing (BIRRP) program to calculate the MT response (Chave and Thomson, 2004). We also applied the remote reference processing to obtain the estimation of MT response (Gamble et al., 1979). We used the magnetic field data obtained at Sukumo Observatory, western part of Shikoku Island, Japan, and/or the ONT-308 site at Noto Peninsula, Japan, as a reference.

Table 1 The details of MT sites on Sakurajima Island. The E and F suffixes on the Site ID indicate electric field and full-component sites, respectively.

Site ID	Latitude (°N)	Longitude (°E)	Elevation (m)	Dipole Length (m)		Recording Period
				N-S	E-W	
SKJ001-E	31.617	130.633	52	20	20	2024/11/20 - 2024/12/12
SKJ002-E	31.620	130.648	40	20	17	2024/10/29 - 2024/11/19
SKJ003-E	31.622	130.668	76	20	20	2024/10/29 - 2024/11/19
SKJ004-F	31.621	130.687	38	20	20	2024/10/29 - 2024/11/19
SKJ005-E	31.620	130.698	25	20	20	2024/10/29 - 2024/11/19
SKJ006-E	31.615	130.693	81	20	20	2024/12/12 - 2025/01/06
SKJ007-F	31.607	130.622	69	20	20	2024/10/29 - 2024/11/19
SKJ008-E	31.610	130.654	279	20	20	2024/11/19 - 2024/12/10
SKJ009-F	31.604	130.638	368	20	20	2024/11/19 - 2024/12/10
SKJ010-F	31.606	130.675	359	20	20	2024/12/10 - 2025/01/06
SKJ011-F	31.607	130.703	65	20	20	2024/10/30 - 2024/11/20
SKJ012-E	31.600	130.650	682	18	15	2024/11/19 - 2024/12/10
SKJ013-F	31.599	130.664	634	20	20	2024/11/20 - 2025/01/07
SKJ014-E	31.604	130.689	132	20	20	2024/12/11 - 2025/01/06
SKJ015-E	31.593	130.609	28	20	20	2024/10/30 - 2024/11/19
SKJ016-F	31.594	130.622	203	20	20	2024/11/18 - 2024/12/10
SKJ017-F	31.593	130.635	389	20	20	2024/10/30 - 2024/12/09
SKJ018-F	31.596	130.694	104	20	20	2024/12/11 - 2025/01/06
SKJ019-F	31.586	130.639	485	20	20	2024/11/20 - 2025/01/07
SKJ020-F	31.588	130.688	122	20	20	2025/01/07 - 2025/02/26
SKJ021-E	31.590	130.708	55	17	20	2024/11/19 - 2024/12/11
SKJ022-E	31.582	130.626	219	17	20	2024/11/18 - 2024/12/10
SKJ023-E	31.582	130.700	108	20	20	2024/12/11 - 2025/01/06
SKJ024-F	31.575	130.605	9	20	20	2024/12/10 - 2025/01/06
SKJ025-F	31.577	130.616	43	20	20	2024/10/30 - 2024/11/18
SKJ026-F	31.578	130.639	329	20	20	2024/11/20 - 2024/12/09
SKJ027-E	31.570	130.640	296	20	20	2024/12/10 - 2025/01/06
SKJ028-E	31.566	130.628	82	20	17	2024/11/18 - 2024/11/25
SKJ029-F	31.569	130.684	193	20	20	2025/01/07 - 2025/02/19
SKJ030-F	31.569	130.709	39	20	20	2024/10/29 - 2024/11/19
SKJ031-E	31.558	130.624	24	20	20	2024/10/30 - 2024/11/18
SKJ032-E	31.560	130.649	196	20	20	2024/12/10 - 2025/03/11
SKJ033-F	31.563	130.676	108	20	19	2024/12/12 - 2025/01/08
SKJ034-E	31.566	130.710	38	20	20	2024/10/30 - 2024/11/18
SKJ035-E	31.547	130.679	26	20	20	2024/12/09 - 2025/01/06

The phase tensor analysis (Caldwell et al., 2004) was calculated from the impedance tensor to assess the dimensionality of the structure. It is graphically represented by an ellipse. A circular shape means the structure is dominated by a 1D distribution. Meanwhile, an ellipsoidal shape means the structure is dominated by a 2D or 3D distribution. Moreover, we evaluate the induction vector from the vertical and horizontal magnetic fields. The induction arrow direction will denote the presence of a good conductor, and its length shows the resistivity contrast (Parkinson, 1962).

The 1D inversion was processed using the Occam algorithm (Constable et al., 1987). We estimated the 1D model from the determinant of the impedance tensor (Z_{det}) using Eq. 1 (Berdichevsky et al., 1980).

$$Z_{det} = \sqrt{Z_{xx}Z_{yy} - Z_{xy}Z_{yx}} \qquad (1)$$

Based on Eq. 1, we only performed 1D inversion at full component sites that record the electric and magnetic fields. This inversion process will produce the resistivity sounding curve beneath each site.

3. Results and Discussion

Broadband MT data were collected in the period range 0.0027 - 910.2222 s at 35 sites. The MT phase tensor was used to evaluate the subsurface dimensionality regardless of the galvanic distortion. The dimensionality is assessed based on the principal axes that depict the ellipse shape and skew angle (β) value. The 1D structure is indicated by a circular shape and β values close to zero. Meanwhile, an ellipse shape with small β values ($\beta<\pm3^{o}$) denotes a 2D structure, and $\beta>\pm3^{o}$ is considered a 3D structure (Caldwell et al., 2004). The phase tensor was plotted with the real induction arrows in Fig. 2. At short periods of 0.010 s, most of the phase tensors show circular shapes with skewness close to zero, which suggests the 1D resistivity structures. At periods of > 7.111 s, most of the phase tensor shows ellipse shapes with large skewness values, indicating the influence of 2D or 3D structures. The phase tensors are mainly aligned in the Northeast - Southwest direction, reflecting the main structure on Sakurajima Island. However, at 7.111 s, some sites in the westward of Sakurajima Island show a different structure orientation aligned in the North - South and West/Northwest - East/Southeast directions.

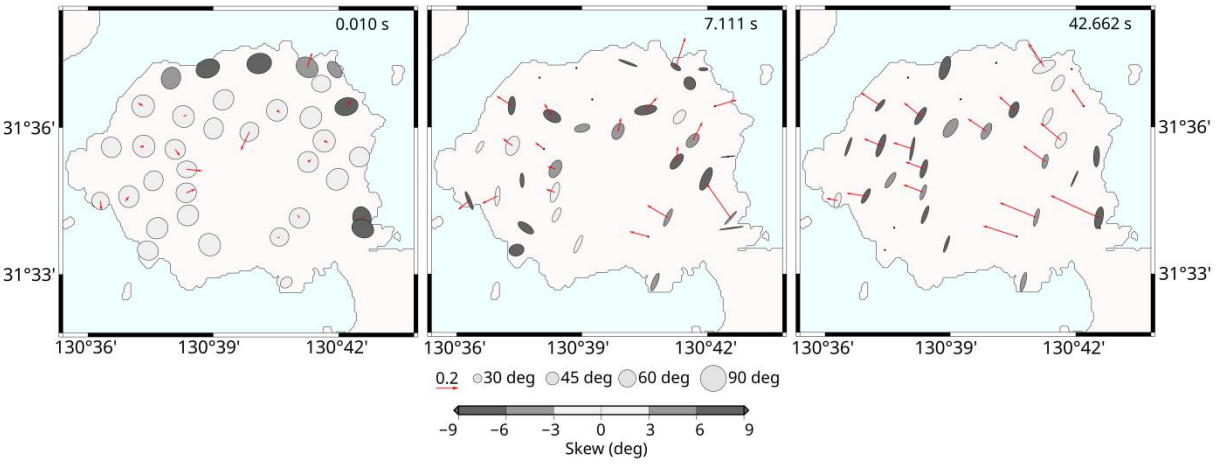

Fig. 2 Distribution of phase tensor ellipses and real induction arrows for periods of 0.01 s, 7.111 s, and 42.662 s. The colors of the ellipses depict the skewness values. The real parts of the induction vectors are plotted according to Parkinson's theorem.

The Parkinson's induction arrow at a short period represents the local conductor in the survey area. Around the Sakurajima volcano, the induction arrows at 0.010 s point to the center of the volcano, indicating a good conductor or the topography effect of the volcano. At periods of 7.111 s, most of

the induction arrows point to the Northeast and Northwest - West directions. We assume that the Northeast induction arrows are related to the main magma reservoir in the Aira caldera (Hidayati et al., 2007). The induction arrows of two sites in the southeastern part of Sakurajima Island indicate a good conductor around Minamidake or Showa crater. Meanwhile, the induction arrows in the western part of Sakurajima Island, which pointed to Northwest - West, may be caused by local sea effect from Kagoshima Bay. At longer periods of 42.662 s, all of the induction vector points to the Northwest - West, indicating the regional conductive area. Hata et al. (2017) that observed the regional structure of the Kyushu Islands also showed the same direction of induction towards the Northwest - West at a period of 40 s and assumed there is a strong conductor in the East China Sea.

The magnetotelluric data were inverted using the Occam 1D inversion code to find the smoothest model that fit the data (Constable et al., 1987). We set the initial half-space resistivity to 100 Ωm. The samples of the 1D resistivity model calculated from the determinant of the impedance tensor are shown in Fig. 3. SKJ013 is located north of Kitadake crater, and SKJ019 is located westward between Kitadake and Minamidake craters. Meanwhile, SKJ026 and SKJ029 are located in the western and southeastern parts of Minamidake and Showa craters, respectively. The 1D models in Fig. 3 show a similar characteristic of resistivity changes. High resistivity is observed near the surface. Then, sharp decreases in resistivity occur at several depths. We estimate that these conductive zones are related to the magmatic system, as reported from tilt and strain observations (Hotta and Iguchi, 2021).

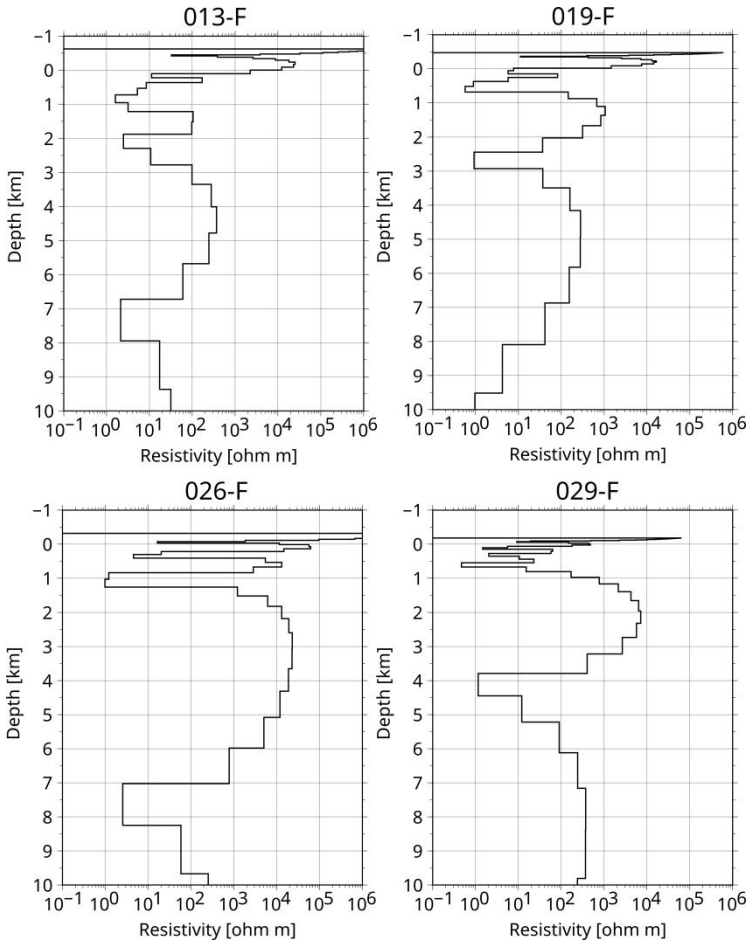

Fig. 3 The resistivity sounding curves for sites SKJ013, SKJ019, SKJ026, and SKJ029 calculated from the determinant of the impedance tensor. The negative value in depth means the position is above sea level.

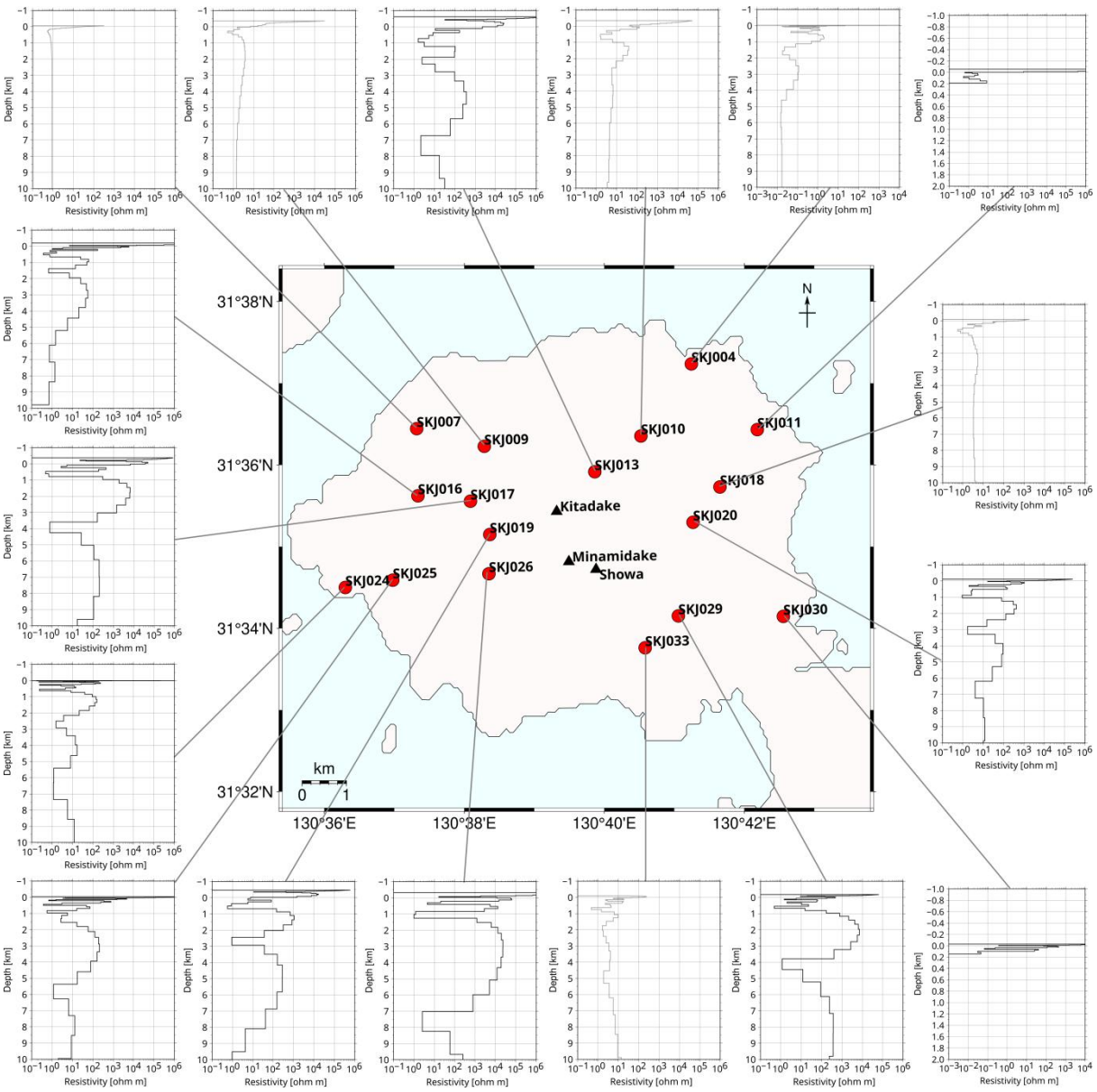

Fig. 4 The resistivity sounding curves of all full-component MT sites on Sakurajima Island. The black and gray curves indicate reliable and unreliable 1D results, respectively. Meanwhile, the negative value in depth means the position is above sea level.

Fig. 4 represents the 1D resistivity model of all full-component MT sites. We observe that almost all sites have high resistivity near the surface, then drop significantly, and the resistivity increases again. These characteristics correlate with Sakurajima's magmatism. The resistivity sounding curves at sites SKJ011 and SKJ030 only had a shallow depth resolution because we only used high-frequency data for the inversion process. Meanwhile, the resistivity sounding curves in gray color indicate the unreliable 1D models since they appear insensitive to resistivity changes with depth. It could be caused by the influence of noise at low frequencies that causes inaccurate resistivity models at certain depths. Our results demonstrate that 1D models provide a preliminary estimation of the subsurface structure on Sakurajima Island. However, to obtain more detailed subsurface imaging from all observation sites, we will perform the 2D and 3D modeling in the future.

4. Conclusions

The subsurface imaging at Sakurajima Island

was carried out using broadband MT data in the frequency range of 0.001 - 400 Hz. The MT data analyses were performed to reveal an initial overview of the Sakurajima volcanic system. We found that the Sakurajima main structure shows a Northeast - Southwest trend and 2D/3D effect from the phase tensor analysis. In addition, the induction vectors at 7.111 s indicate the presence of conductive zones in the Northeast of Sakurajima and around Minamidake and/or Showa craters. The 1D resistivity models at 17 full-component sites were obtained using the Occam inversion algorithm. The observed conductive zones around the craters are thought to be related to the Sakurajima magmatism. However, to confirm the 1D result and further analysis, we need to carry out the 2D and 3D inversions.

Acknowledgements

The authors appreciate the landowners, heads of each district, and local administrative organizations for their assistance and permission to use their area for the survey. The MT instruments were provided by collaborative research projects at the Disaster Prevention Research Institute of Kyoto University, and some additional magnetic sensors were supported by Geothermal Science of Kyoto University's Graduate School of Science. We were supported by the Ministry of Education, Culture, Sports, Science and Technology (MEXT) of Japan, under its Third Earthquake and Volcano Hazards Observation and Research Program. This study was a part of CND's doctoral program funded by the Indonesian Endowment Fund for Education (LPDP).

References

Aizawa, K., Koyama, T., Hase, H., and Makoto, U. (2013): 3-D Resistivity Structure of Sakurajima Volcano and its temporal change from Magnetotelluric Continuous Observation. http://www.svo.dpri.kyoto-u.ac.jp/H25sakura/11aizawa.pdf

Caldwell, T. G., Bibby, H. M., and Brown, C. (2004): The magnetotelluric phase tensor. Geophysical Journal International, Vol. 158, No. 2, pp. 457-469.

Chave, A. D. and Thomson, D. J. (2004): Bounded influence magnetotelluric response function estimation. Geophysical Journal International, Vol. 157, No. 3, pp. 988-1006.

Constable, S. C., Parker, R. L., and Constable, C. G. (1987): Occam's inversion: A practical algorithm for generating smooth models from electromagnetic sounding data. Geophysics, Vol. 52, No. 3, pp.289-300.

Constable, S. C., Parker, R. L., and Constable, C. G. (1987): Occam's inversion: A practical algorithm for generating smooth models from electromagnetic sounding data. Geophysics, Vol. 52, No. 3, pp. 289-300.

Gamble, T.D., Goubau, W.M. and Clarke, J. (1979): Magnetotellurics with a remote magnetic reference. Geophysics, Vol. 44, No. 1, pp. 53-68.

Hata, M., Uyeshima, M., Handa, S., Shimoizumi, M., Tanaka, Y., Hashimoto, T., Kagiyama, T., Utada, H., Munekane, H., Ichiki, M., and Fuji-ta, K. (2017): 3-D electrical resistivity structure based on geomagnetic transfer functions exploring the features of arc magmatism beneath Kyushu, Southwest Japan Arc. Journal of Geophysical Research: Solid Earth, Vol. 122, No. 1, pp. 172-190.

Hidayati, S., Ishihara, K., and Iguchi, M. (2007): Volcano-tectonic earthquakes during the stage of magma accumulation at the Aira caldera, southern Kyushu, Japan. Bulletin of the Volcanological society of Japan, Vol. 52, No. 6, pp. 289-309.

Hill, G.J., Bibby, H.M., Ogawa, Y., Wallin, E.L., Bennie, S.L., Caldwell, T.G., Keys, H., Bertrand, E.A., and Heise, W. (2015): Structure of the Tongariro Volcanic system: Insights from magnetotelluric imaging. Earth and Planetary Science Letters, Vol. 432, pp.115-125.

Hotta, K and Iguchi, M. (2021): Tilt and strain change during the explosion at Minami-dake, Sakurajima, on November 13, 2017. Earth, Planets and Space, Vol. 73, No. 1, p.70.

Kanda, W., Yamazaki, T., Ogawa, Y., Hashimoto, T., Sakanaka, S., Aizawa, K., Takakura, S., Koyama, T., Yamada, K., Kobayashi, T., and Komori, S. (2013): Shallow Resistivity Structure of Sakurajima Volcano Revealed by Audio-frequency Magnetotellurics (Special

Section Sakurajima Special Issue). Bulletin of the Volcanological Society of Japan, Vol. 58, No.1, pp. 251-267.

Parkinson, W. D. (1962): The influence of continents and oceans on geomagnetic variations. Geophysical Journal International, Vol.6, No. 4, pp.441-449.

Permana, T., Nishimura, T., Nakahara, H., and Shapiro, N. (2022): Classification of volcanic tremors and earthquakes based on seismic correlation: Application at Sakurajima volcano, Japan. Geophysical Journal International, Vol. 229, No. 2, pp. 1077-1097.

Simpson, F. and Bahr, K. (2005): Practical magnetotellurics. Cambridge University Press.

Yamaoka, K., Miyamachi, H., Watanabe, T., Kunitomo, T., Michishita, T., Ikuta, R., and Iguchi, M. (2014): Active monitoring at an active volcano: amplitude-distance dependence of ACROSS at Sakurajima Volcano, Japan. Earth, Planets and Space, Vol. 66, No. 1, p.32.

(Received August 26, 2025)